*Carbon* 1970, Vol. 8, pp. 211–226. Pergamon Press. Printed in Great Britain

# THEORY OF THERMAL EXPANSION OF A GRAPHITE CRYSTAL IN THE SEMI-CONTINUUM MODEL

**B. T. KELLY**
U.K.A.E.A. Reactor Materials Laboratory, Culcheth, Nr. Warrington, Lancs, England

**and**

**P. L. WALKER, Jr.**
Department of Materials Science, Pennsylvania State University, University Park, Penna. 16802, U.S.A.

(*Received* 11 *September* 1969)

**Abstract**—A new theory of the principal thermal expansion coefficients of a graphite crystal is derived using the lattice dynamics obtained by Komatsu. The theory is compared with new data on the low temperature thermal expansion coefficients of very highly oriented pyrolytic graphite and high temperature X-ray data. Values of some of the lattice anharmonic coefficients are estimated.

## 1. INTRODUCTION

Accurate measurements of the principal thermal expansion coefficients of the graphite lattice obtained by X-ray and direct methods are available over a wide range of temperatures[1–4]. The principal expansion coefficients have also been derived from data on polycrystalline graphite[5–7] and very perfect pyrolytic graphite[8, 9].

The graphite crystal has symmetry $D_h^6$ and therefore two independent expansion coefficients, which may be measured parallel to the hexagonal axis (or $c$-axis) and in any direction perpendicular to it; these coefficients are denoted by $\alpha_c$ and $\alpha_a$ respectively. The coefficient $\alpha_c$ is positive at all temperatures, but $\alpha_a$ is more complicated. At temperatures below 400°C, $\alpha_a$ is negative, but it is positive at temperatures greater than 400°C. In general the magnitude of $\alpha_a$ is much less than that of $\alpha_c$.

The experimental data have been analysed in the past using a theory due to Riley[10]. The theory assumes two lattice vibrational modes polarised respectively parallel and perpendicular to the basal planes and known as in-plane vibrations and out-of-plane vibrations respectively. Each of these modes is assumed to be described by a Debye model [11] with a characteristic temperature. The out-of-plane waves possess a Debye temperature of 760°K and the in-plane vibrations a Debye temperature of 2200°K, the values being derived from specific heat data on the same assumptions.

Recent work has shown that the specific heat[12], thermal conductivity[13] and thermal vibration amplitudes of carbon atoms[14] can be understood in terms of the lattice dynamics due to Komatsu[12]. It is appropriate to examine the theory of the principal thermal expansion coefficients of a graphite crystal using the same lattice dynamics. Calculated values of elastic coefficients and anharmonicities using interatomic potentials can be compared with experimental values and are useful tests of the validity of such potentials.

## 2. THEORY

Consider a unit cube of the graphite crystal with one face parallel to the basal planes. The free energy of the crystal in a dilated state, i.e. no shear strains, induced thermally, is:

$$F = U_0 + \tfrac{1}{2}(e_{xx}^2 + e_{yy}^2)C_{11} + \tfrac{1}{2}C_{33}e_{zz}^2 + C_{12}e_{xx}e_{yy} + C_{13}e_{zz}(e_{xx} + e_{yy}) + kT\sum_{\nu_p} \ln\left[1 - \exp\left(-\frac{h\nu_p}{kT}\right)\right] \quad (1)$$

where $U_0$ is the energy/unit volume at absolute zero in the unstrained state.

$C_{11}$, $C_{12}$, $C_{13}$, $C_{33}$ and $C_{44}$ are the usual elastic constants.

$e_{lm}$ are the elements of the strain tensor in a Cartesian co-ordinate system with the $Z$ axis coincident with the hexagonal or $c$-axis of the crystal.

$\nu_p$ is the vibration frequency of the p'th vibrational mode.

$k$ is Boltzmann's constant.

$T$ is the absolute temperature in °K.

The summation over frequencies and modes is to be taken over the first Brillouin zone [13].

The termal expansion of a hexagonal crystal produces strains $e_{zz}$ and $e_{xx} = e_{yy}$. The principal thermal expansion coefficients are, therefore

$$\alpha_c = \left(\frac{\partial e_{zz}}{\partial T}\right)$$

$$\alpha_a = \left(\frac{\partial e_{xx}}{\partial T}\right) = \left(\frac{\partial e_{yy}}{\partial T}\right). \quad (2)$$

At equilibrium, the free energy $F$ in equation (1) is a minimum with respect to all variables. Differentiating (1) in turn with respect to $e_{zz}$ and $e_{xx}$ and equating each to zero, leads to

$$C_{33}e_{zz} + C_{13}(e_{xx} + e_{yy}) - \sum_{\nu,p} \frac{h\nu_p}{[\exp(h\nu_p/kT) - 1]}[\gamma_p]_{zz} = 0$$

$$C_{11}e_{xx} + C_{12}e_{yy} + C_{13}e_{zz} - \sum_{\nu,p} \frac{h\nu_p}{[\exp(h\nu_p/kT) - 1]}[\gamma_p]_{xx} = 0 \quad (3)$$

where $[\gamma_p]_{ii} = -\frac{1}{\nu_p}\left(\frac{\partial \nu_p}{\partial e_{ii}}\right)$.

Solving the equation (3) for $e_{zz}$ and $e_{xx}$ (remembering $e_{xx} = e_{yy}$) and differentiating with respect to $T$ gives

$$\frac{de_{zz}}{dT} = \alpha_c = \frac{(C_{11} + C_{12})}{C_{33}(C_{11} + C_{13}) - 2C_{13}^2} \sum_{\nu,p} k\left(\frac{h\nu_p}{kT}\right)^2 \frac{\exp[h\nu_p/kT] \cdot [\gamma_p]_{zz}}{\{\exp[h\nu_p/kT] - 1\}^2} - \frac{2C_{13}}{C_{33}(C_{11} + C_{12}) - 2C_{13}^2} \sum_{\nu,p} k\left(\frac{h\nu_p}{kT}\right)^2 \frac{\exp[h\nu_p/kT] \cdot [\gamma_p]_{xx}}{\{\exp[h\nu_p/kT] - 1\}^2} \quad (4)$$

$$\frac{de_{zz}}{dT} = \alpha_a = \frac{C_{33}}{C_{33}(C_{11} + C_{12}) - 2C_{13}^2} \sum_{\nu,p} k\left(\frac{h\nu_p}{kT}\right)^2 \frac{\exp[h\nu_p/kT] \cdot [\gamma_p]_{xx}}{\{\exp[h\nu_p/kT] - 1\}^2} - \frac{C_{13}}{C_{33}(C_{11} + C_{12}) - 2C_{13}^2} \sum_{\nu,p} k\left(\frac{h\nu_p}{kT}\right)^2 \frac{\exp[h\nu_p/kT] \cdot [\gamma_p]_{zz}}{\{\exp[h\nu_p/kT] - 1\}^2}. \quad (5)$$

In hexagonal crystals the elastic constants $C_{IJ}$ are related to the elastic compliances $S_{IJ}$ by

$$S_{13} = C_{13}/X,\ S_{11} + S_{12} = C_{33}/X,$$
$$S_{33} = (C_{11} + C_{12})/X$$

where $X = C_{33}(C_{11} + C_{12}) - 2C_{13}^2$.

Substitution of these relations into (4) and (5) gives finally:-

$$\alpha_c = S_{33}k \sum_{\nu,p} \left(\frac{h\nu_p}{kT}\right)^2 \frac{\exp(h\nu_p/kT) \cdot [\gamma_p]_{zz}}{\{\exp(h\nu_p/kT) - 1\}^2} + 2S_{13}k \sum_{\nu,p} \left(\frac{h\nu_p}{kT}\right)^2 \frac{\exp(h\nu_p/kT) \cdot [\gamma_p]_{xx}}{\{\exp(h\nu_p/kT) - 1\}^2} \quad (6)$$

and

$$\alpha_a = (S_{11} + S_{12}) \cdot k \sum_{\nu,p} \left(\frac{h\nu_p}{kT}\right)^2 \frac{\exp(h\nu_p/kT) \cdot [\gamma_p]_{xx}}{\{\exp(h\nu_p/kT) - 1\}^2} + S_{13} \cdot k \sum_{\nu,p} \left(\frac{h\nu_p}{kT}\right)^2 \frac{\exp(h\nu_p/kT) \cdot [\gamma_p]_{zz}}{\{\exp(h\nu_p/kT) - 1\}^2}. \quad (7)$$

Some simplification of these expressions is possible using the elastic compliances of a graphite crystal measured by Soule *et al*[15], given in Table 1.

Clearly (6) can be replaced by

$$\alpha_c = S_{33}k \sum_{\nu,p} \left(\frac{h\nu_p}{kT}\right)^2 \frac{\exp(h\nu_p/kT) \cdot [\gamma_p]_{zz}}{\{\exp(h\nu_p/kT) - 1\}}. \quad (8)$$

In order to make further progress we must consider the lattice vibration spectrum of graphite. The unit cell of the graphite lattice contains four atoms. There are, therefore, twelve vibrational modes to be considered, three acoustic modes and nine optical modes. The most detailed calculations of the spectrum are due to Yoshimori and Kitano[16] who used the Born-Von Karman method, but for most purposes the semi-continuum model due to Komatsu[12] is adequate. The optical modes can for most purposes be neglected, since they require high temperature for their excitation. The three acoustic modes in Komatsu's[12] model comprise one polarised parallel to the hexagonal axis (out-of-plane mode) and two polarised parallel to the basal planes (in-plane transverse and in-plane longitudinal modes). The frequencies of the three acoustic modes in this model are given by:

$$\tau = (C_{44}/\rho)^{1/2}$$

$\mu^2 = (C_{33}/\rho d^2)$

$\delta$ measures the resistance of a layer to bending

$\rho$ is the density.

Equation (9) leads to the following expressions for the anharmonicities $[\gamma_p]_{ii}$.†

$$[\gamma_1]_{ii} = -\nu_1^{-1}\left[\frac{\partial \nu_1}{\partial e_{ii}}\right] = -\frac{1}{2}\left(\frac{C_{11}}{\rho} \cdot \sigma_a^2 + \frac{C_{44}}{\rho\pi^2 d^2}\sin^2 \pi d\sigma_z\right)^{-1}\left\{\frac{\sigma_a^2}{\rho}\left(\frac{\partial C_{11}}{\partial e_{ii}}\right) + \frac{\sin^2 \pi d\sigma_z}{\rho\pi^2 d^2}\left(\frac{\partial C_{44}}{\partial e_{ii}}\right)\right\}$$

$$[\gamma_2]_{ii} = -\frac{1}{2}\left(\frac{1}{2}\frac{(C_{11} - C_{12})}{\rho}\sigma_a^2 + \frac{C_{44}}{\rho\pi^2 d^2}\sin^2 \pi d\sigma_z\right)^{-1}\left\{\frac{\sigma_a^2}{\rho}\frac{1}{2}\left|\left(\frac{\partial C_{11}}{\partial e_{ii}}\right) - \frac{\partial C_{12}}{\partial e_{ii}}\right| + \frac{\sin^2 \pi d\sigma_z}{\rho\pi^2 d^2}\left(\frac{\partial C_{44}}{\partial e_{ii}}\right)\right\} \quad (10)$$

$$[\gamma_3]_{ii} = -\frac{1}{2}\left(4\pi^2\delta^2\sigma_a^4 + \frac{\mu^2}{\pi^2}\sin^2 \pi d\sigma_z + \tau\sigma_a^2\right)^{-1} \times \left\{8\pi^2\delta\left(\frac{\partial \delta}{\partial e}\right)_{ii}\sigma_a^4 + \frac{\sin^2 \pi d\sigma_z}{\rho\pi^2 d^2}\left(\frac{\partial C_{33}}{\partial e_{ii}}\right) + \left(\frac{\partial C_{44}}{\partial e_{ii}}\right)\frac{\sigma_a^2}{\rho}\right\}.$$

| | |
|---|---|
| In-plane longitudinal mode | $\nu_1 = \left[V_L^2\sigma_a^2 + \frac{\tau}{\pi^2 d^2}\sin^2 \pi d\sigma_z\right]^{1/2}$ |
| In-plane transverse mode | $\nu_2 = \left[V_T^2\sigma_a^2 + \frac{\tau}{\pi^2 d^2}\sin^2 \pi d\sigma_z\right]^{1/2}$ (9) |
| Out-of-plane mode | $\nu_3 = \left[4\pi^2\delta^2\sigma_a^4 + \frac{\mu^2}{\pi^2}\sin^2 \pi d\sigma_z + \tau\sigma_a^2\right]^{1/2}$ |

where $\sigma_a$, $\sigma_z$ are the wave number components parallel and perpendicular to the basle planes respectively.

$d = (3{\cdot}3535$ Å$)$ is the inter-layer spacing

$V_L = (C_{11}/\rho)^{1/2}$ is the longitudinal elastic wave velocity

$V_T = (\frac{1}{2}(C_{11} - C_{12})/\rho)^{1/2}$ is the transverse elastic wave velocity

Expressions (10) show that in each mode the $[\gamma_p]_{ii}$ depend upon the relative magnitude of $\sigma_a$ and $\sigma_z$, the wave number components. In order to proceed further we require the coefficients of the effects of strain on elastic moduli. Some simplication is

†See note added in proof

achieved by the previous observation [13] that only the first terms in each of the first brackets in equation (10) are important above 200°K, it is not however certain that the same holds in the second brackets. The only reported measurement of variations in elastic moduli with strain is due to Blakeslee and Proctor (quoted by Reynolds [15]). These authors give

$$\frac{1}{C_{33}} \cdot \frac{dC_{33}}{d\sigma_{zz}} = -10{\cdot}9 \times 10^{-11}\ \text{cm}^2/\text{dyne}$$

or $(\partial C_{33}/\partial e_{zz}) = -14{\cdot}5 \times 10^{12}$ dynes/cm$^2$ obtained from measurements on pyrolytic graphite of high perfection. However some values may also be obtained theoretically. It has been shown by Girifalco and Lad [17], Agranovich and Semenov [18] and Crowell [19], that Lennard–Jones potentials between atoms in separate layers give good results for the cohesive energy and compressibility of a graphite crystal. Recently Drickamer *et al.* [10] have shown that the Girifalco-Lad potential can account for the non-linearity of strain $e_{zz}$ under high compressive strain (~ 15 per cent), very well; it may therefore be adequate to calculate $C_{33}$, $C_{44}$, $(\partial C_{33}/\partial e_{zz})$ and $(\partial C_{44}/\partial e_{zz})$. Kelly and Duff [21] have calculated $C_{33}$ and $\partial C_{33}/\partial e_{zz}$ using Girifalco and Lad's data, and also $C_{33}$, $C_{44}$ and $\partial C_{33}/\partial e_{zz}$, using the Agranovich and Semenov method (considering only interactions between adjacent layers). In the same paper an estimate is made of $(\partial C_{44}/\partial e_{zz})$.

Table 2 summarises the results of calculations and experiment.

It is clear that the potential gradient concerning strain $e_{zz}$ is apparently reasonable but that the shear constant $C_{44}$ and change of $C_{33}$ with $e_{zz}$ are less satisfactory. Similar difficulties are noted by Komatsu [12] and Dolling and Brockhouse [23].

We now turn to the comparison of theory and experiment.

## 3. COMPARISON OF THEORY AND EXPERIMENT

It is appropriate to consider the principal thermal expansion coefficients $\alpha_c$ and $\alpha_a$ respectively, separately:-

### 3.1 *Hexagonal axis thermal expansion coefficient* $\alpha_c$

Experimental data for $\alpha_c$ as a function of temperature on very perfect graphite extend

Table 1. Elastic compliances and moduli of a graphite crystal

| Elastic constant | cm$^2$/dyne | Elastic modulus | dyne/cm$^2$ |
|---|---|---|---|
| $S_{11}$ | $0{\cdot}98 \pm 0{\cdot}03 \times 10^{-13}$ | $C_{11}$ | $106 \pm 2 \times 10^{11}$ |
| $S_{12}$ | $-0{\cdot}16 \pm 0{\cdot}06 \times 10^{-13}$ | $C_{12}$ | $18 \pm 2 \times 10^{11}$ |
| $S_{13}$ | $-0{\cdot}33 \pm 0{\cdot}08 \times 10^{-13}$ | $C_{13}$ | $1{\cdot}5 \pm 0{\cdot}5 \times 10^{11}$ |
| $S_{33}$ | $27{\cdot}4 \pm 1{\cdot}0 \times 10^{-13}$ | $C_{33}$ | $3{\cdot}65 \pm 0{\cdot}1 \times 10^{11}$ |
| $S_{44}$ | $0{\cdot}25 \times 10^{-10}$ | $C_{44}$ | $4 \times 10^{10}$ |

Table 2. Calculated properties of graphite crystals using Lennard–Jones interatomic potentials

| Method of calculation | A–A Stacking fault energy | Parameter values $C_{33}$ (dynes/cm$^2$) | $C_{44}$ (dynes/cm$^2$) | $(\partial C_{33}/\partial e_{zz})$ (dynes/cm$^2$) |
|---|---|---|---|---|
| Girifalco–Lad | | $3{\cdot}65 \times 10^{11}$ | | $-6{\cdot}04 \times 10^{12}$ |
| Agranovich–Semenov | 55 | $3{\cdot}86 \times 10^{11}$ | $0{\cdot}23 \times 10^{10}$ | $-7{\cdot}27 \times 10^{12}$ |
| Expt. | 38 [22] | $3{\cdot}65 \times 10^{11}$ | $4 \times 10^{10}$ | $-14{\cdot}5 \times 10^{12}$ |

from 25°K to 2900°K, obtained by direct measurement and X-ray methods[1–9]. First, as an approximation, assume the $\gamma$'s are independent of wave number and, therefore, of temperature as in the usual Gruneisen theory. Then equation (8) can be written.

$$\alpha_c = S_{33}\rho[C_1(T)\,[\gamma_1]_{zz} + C_2(T)\,[\gamma_2]_{zz} + C_3(T)\,[\gamma_3]_{zz}] \qquad (11)$$

where $C_1(T)$, $C_2(T)$ and $C_3(T)$ are the acoustic mode specific heat contributions.

In an earlier theory, Riley[10] further made the plausible assumption that the hexagonal axis coefficient is solely determined by the out-of-plane vibrations, whence (11) is

$$\alpha_c = S_{33}\rho\,[\gamma_3]_{zz}C_3(T). \qquad (12)$$

The values of $[\gamma_3]_{zz}$ can then be calculated from the $\alpha_c$ data and the $C_3(T)$ values due to Komatsu[12] and Komatsu and Nagamiya [24]. The results are shown in Table 3, below and in Fig. 1.

Table 3. Estimated values of $[\gamma_3]_{zz}$ from equation (12)

| Temp. (°K) | Sp. heat $C_3(T)$* (cal/gm/°C) | Thermal exp. coefficient ($\alpha_c$°K$^{-1}$) | $[\gamma_3]_{zz}$ |
|---|---|---|---|
| 45 | 0·00726 | $7{\cdot}5\times10^{-6}$ | 4·0 |
| 100 | 0·0256 | 17·4 | 2·6 |
| 150 | 0·0428 | 22·4 | 2·0 |
| 200 | 0·0586 | 25·0 | 1·67 |
| 250 | 0·0736 | 26·8 | 1·40 |
| 300 | 0·0842 | 27·0 | 1·23 |
| 273 | 0·098 | 25·0 | 0·98 |
| 523 | 0·136 | 25·9 | 0·73 |
| 773 | 0·150 | 27·2 | 0·69 |
| 1,023 | 0·160 | 28·5 | 0·68 |
| 1,273 | 0·165 | 29·7 | 0·69 |
| 1,773 | 0·171 | 32·0 | 0·69 |
| 2,273 | 0·172 | 34·2 | 0·76 |
| 2,773 | 0·173 | 36·2 | 0·80 |

The apparent value of $[\gamma_3]_{zz}$ is approximately constant above 523°K, but rises sharply below 300°K. The value of 0·7 at high temperatures is unusually low. This behaviour can be understood qualitatively in terms of equation (12), and the third of equations (10). Previous work[12, 14] has shown that for a number of thermal properties the graphite may be regarded as two dimensional above 200°K. The first term in the first bracket in equation (10) is the only significant one; if the first term in the second bracket also dominates at high temperatures then

$$[\gamma_3]_{zz} \to \delta^{-1}[\partial\delta/\partial e_{zz}] \qquad (13)$$

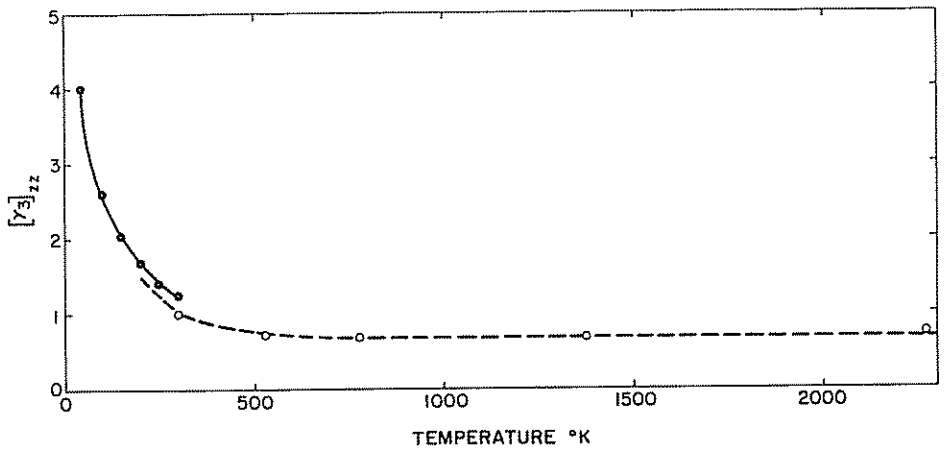


Fig. 1. Anharmonic coefficient for out-of-plane vibrations in first approximation.

at high temperatures. $\delta$ is essentially a property of the planar covalent bonds, i.e. a bond bending constant and it is not surprising that this is insensitive to $e_{zz}$. At temperatures below 200°K, $C_{33}$ and $C_{44}$ become much more important and are much more sensitive to $e_{zz}$, leading to high $[\gamma_3]_{zz}$ values.

This view is too simple however. In Fig. 2, the ratio of the out-of-plane to in-plane wave

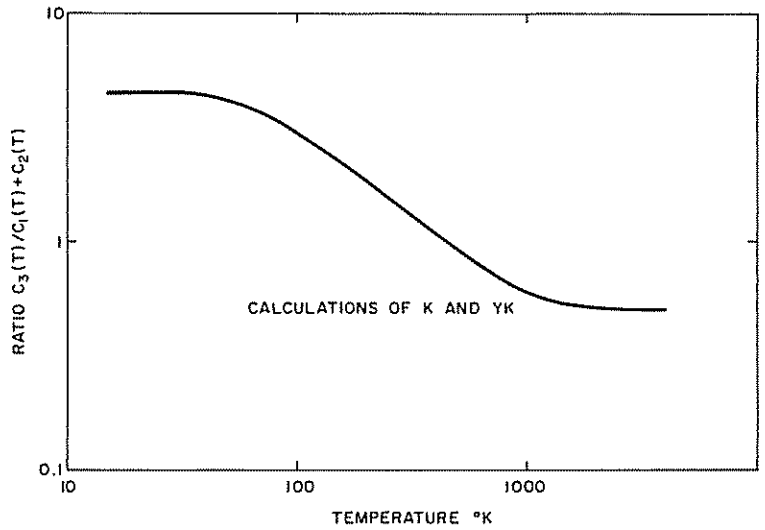


Fig. 2. Ratio of out-of-plane specific heat to in-plane specific heat contributions as a function of temperature.

specific heat components is shown as a function of temperature; above 1500°K the contributions are approximately equal from all three modes. If the in-plane modes can be regarded as two dimensional at high temperatures then

$$[\gamma_1]_{zz} \to \frac{1}{2C_{11}}\left(\frac{\partial C_{11}}{\partial e_{zz}}\right) \text{ and } [\gamma_2]_{zz} \to \frac{1}{2(C_{11}-C_{12})}\cdot\left(\frac{\partial}{\partial e_{zz}}(C_{11}-C_{12})\right).$$

In each case the parameters are changes in the in-plane bonds and thus might be expected to be of similar magnitude. If this surmise is correct all these modes are of roughly equal importance at high temperatures and

$$\frac{1}{2C_{11}}\cdot\left(\frac{\partial C_{11}}{\partial e_{zz}}\right) \approx \frac{1}{2(C_{11}-C_{12})} \times\left(\frac{\partial (C_{11}-C_{12})}{\partial e_{zz}}\right) \approx \frac{1}{\delta}\cdot\left(\frac{\partial \delta}{\partial e_{zz}}\right) \sim 0.2.$$

Figure 2 shows that at low temperatures the out-of-plane mode is much the most important and equation (8) should be a good approximation, summing over out-of-plane modes alone.* If this is correct, then in

*All theoretical calculations refer to the case of constant strain, whereas the data refer to the case of constant stress, as does Col. 2 in Table 2. Bailey and Yates[8] have shown that

$$Cp/Ce_{ii} = 1+\frac{T}{Cp}\alpha_e{}^2 C_{33}$$

and evaluated the correction $(Cp-Ce_{ii})$. The correction is less than 1 per cent and is neglected in this work. The continued use of theoretical specific heat values, implies that no corrections for the electronic heat capacity is necessary.

integral form equation (8) is

$$\alpha_c = -\pi S_{33} k\left(\frac{h}{kT}\right)^2 \int_0^{\sigma_m} \int_{-(1/2d)}^{+(1/2d)} \frac{\sigma_a\left[8\pi^2\delta\sigma_a{}^4(\partial\delta/\partial e_{zz}) + (\partial C_{33}/\partial e_{zz})\dfrac{\sin^2\pi d\sigma_z}{\rho\pi^2 d^2} + (\partial C_{44}/\partial e_{zz})\dfrac{\sigma_a{}^2}{\rho}\right]}{\left\{\exp\left[\dfrac{h}{kT}\left(4\pi^2\delta^2\sigma_a{}^4 + \dfrac{\mu^2}{\pi^2}\sin^2\pi d\sigma_z + \tau\sigma_a{}^2\right)^{1/2}\right] - 1\right\}^2}$$

$$\times \exp\left[\frac{h}{kT}\left(4\pi^2\delta^2\sigma_a{}^4 + \frac{\mu^2}{\pi^2}\sin^2\pi d\sigma_z + \tau\sigma_a{}^2\right)^{1/2}\right] d\sigma_z \,.\, d\sigma_z \qquad (14)$$

where $\sigma_m$ is the equivalent radius of the Brillouin zone[13]. At higher temperatures the right hand side of equation (14) should be compared with the quantity $\alpha_c(T) - 0{\cdot}2S_{33}$-$[C_1(T) + C_2(T)]$ that is $\alpha_c$ corrected for the in-plane contribution (approximately).

Equation (14) has been evaluated numerically for seven cases, for which the parameters are given in Table 4 below. The results are shown in Figs. 3–5 inclusive. The order of magnitude of $(\partial\delta/\partial e_{zz})$ is estimated from $1/\delta(\partial\delta/\partial e_{zz}) \sim 0.2$ and that of $(\partial C_{44}/\partial e_{zz})$ from

$$\left(\frac{\partial C_{44}}{\partial e_{zz}}\right) = \left(\frac{C_{44}}{C_{33}}\right) \cdot \left(\frac{\partial C_{33}}{\partial e_{zz}}\right) = -8{\cdot}11 \times 10^{11} \times \text{dynes/cm}^2$$

(the same interplanar bonds determine $C_{33}$ and $C_{44}$).

In Fig. 3 cases 1, 3 and 2A are compared to obtain an estimate of the effect of changes in $(\partial C_{44}/\partial e_{zz})$, holding the other parameters constant. Comparison of 1 and 3 shows that a factor of three variation produces 10 per cent change in $\alpha_c$. Case 2A shows that a very small change in $(\partial C_{33}/\partial e_{zz})$ can compensate for a large change in $(\partial C_{44}/\partial e_{zz})$. We conclude that $(\partial C_{44}/\partial e_{zz})$ is not a very important factor in determining $\alpha_c$. Figure 4 confirms the sensitivity of $\alpha_c$ at low temperatures to the value of $(\partial C_{33}/\partial e_{zz})$ suggested by case 2A, by comparing cases 1A and 3. Figure 5 shows that the curve is relatively insensitive to $(\partial\delta/\partial e_{zz})$, over a factor of 4 (cases 1, 2, 3A). Case 4 uses the only experimental value of $(\partial C_{33}/\partial e_{zz})$ and yields expansion coefficients much too large. The value of $(\partial C_{33}/\partial e_{zz}) = -7{\cdot}27 \times 10^{12}$ dyne/cm$^2$ is supp rted by the theoretical calculation of Girifalco and Lad[14] as analysed by Kelly and Duff[21], and the high pressure measurements of Drickamer *et al.*[20]. It also gives a reasonable estimate for the expansion coefficient. We therefore assume it to be roughly correct. Figure 5 shows the best fit of theory and experiment at low temperature using the data of Bailey and Yates[8]. The fit is very good indeed showing that the continuum model can account for the low temperature $\alpha_c$ with values.

$$(\partial\delta/\partial e_{zz}) = -1{\cdot}4 \times 10^{-3}\ \text{cm}^2/\text{sec}$$
$$(\partial C_{33}/\partial e_{zz}) = -6 \times 10^{12}\ .\ \text{dynes/cm}^2$$
$$(\partial C_{44}/\partial e_{zz}) = -10^{11}\ .\ \text{dynes/cm}^2$$

although the accuracy on the first and last is not high.

Figure 6 compares this calculation up to 3000°C with the experimental data, in the form of a "probable best curve", normalised on to that of Bailey and Yates[8]. The theoretical curve falls below the experimental one from about 800°K upwards; all of the theoretical calculations for the out-of-plane contribution to $\alpha_c$ have this characteristic flattening at high temperatures. There are three possible reasons for the discrepancy:-

1. The difference is due to the in-plane contribution to $\alpha_c$, that is the correction to equation (14) at high temperature. This is examined in greater detail below.
2. The difference is due to the excitation of optical modes (particularly out-of-plane) at high temperatures. This is not likely to be large enough to account for all of the difference, since the optical modes contribution

Table 4. Parameters used to evaluate out-of-plane contribution to $\alpha_c$

| Case | 1 | 1A | 2 | 2A | 3 | 3A | 4 |
|---|---|---|---|---|---|---|---|
| Parameter | | | | | | | |
| $S_{33}$ cm²/dyne | $27{\cdot}5 \times 10^{-3}$ | | | | | | |
| $\delta$ cm²/sec | $6{\cdot}11 \times 10^{-3}$ | | | | | | |
| $d$ cm | $3{\cdot}35 \times 10^{-8}$ | | | | | | |
| $\rho$ g/cc | 2·26 | | | | | | |
| $\mu^2$ | $140 \times 10^{24}$ | | | | | | |
| $\tau$ | $1{\cdot}77 \times 10^{10}$ | | | | | | |
| $\sigma_m{}^2$ . cm$^{-2}$ | $6{\cdot}05 \times 10^{14}$ | | | | | | |
| $(\partial\delta/\partial e_{zz})$ cm²/sec | $-1{\cdot}4 \times 10^{-3}$ | $-1{\cdot}4 \times 10^{-3}$ | $-4{\cdot}2 \times 10^{-3}$ | $-1{\cdot}4 \times 10^{-3}$ | $-1{\cdot}4 \times 10^{-3}$ | $-1{\cdot}0 \times 10^{-3}$ | $-1{\cdot}4 \times 10^{-3}$ |
| $(\partial C_{33}/\partial_{zz})$ dyne/cm² | $-7{\cdot}27 \times 10^{12}$ | $-6 \times 10^{12}$ | $-7{\cdot}27 \times 10^{12}$ | $-7{\cdot}3 \times 10^{12}$ | $-7{\cdot}27 \times 10^{12}$ | $-7{\cdot}3 \times 10^{12}$ | $-14{\cdot}5 \times 10^{12}$ |
| $(\partial C_{44}/\partial e_{zz})$ dyne/cm² | $-3{\cdot}55 \times 10^{11}$ | $-1 \times 10^{11}$ | $-3{\cdot}55 \times 10^{11}$ | $-1{\cdot}0 \times 10^{10}$ | $-1{\cdot}0 \times 10^{11}$ | $-1{\cdot}0 \times 10^{11}$ | $-7{\cdot}5 \times 10^{11}$ |

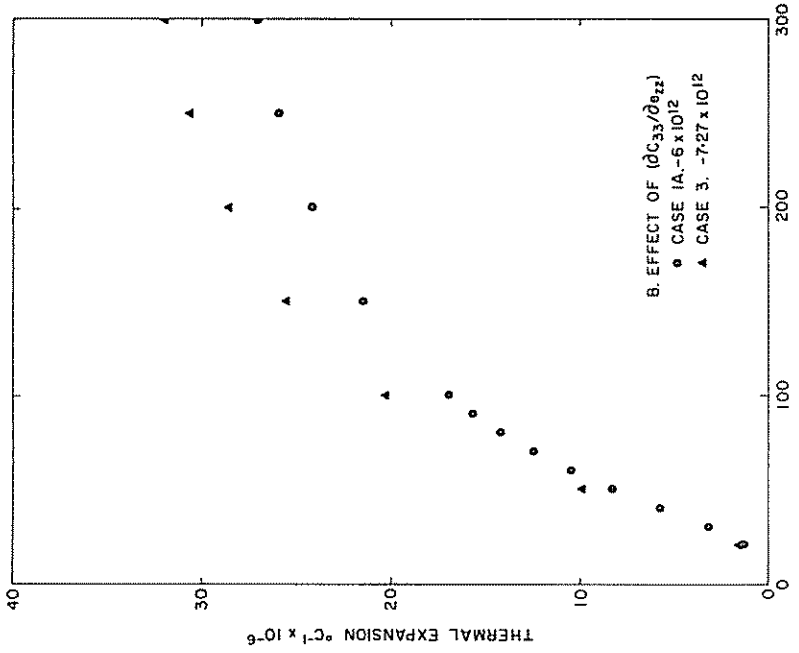


Fig. 4. Comparison of theoretical values of $\alpha_c$. Low temperature. Parametric variation.

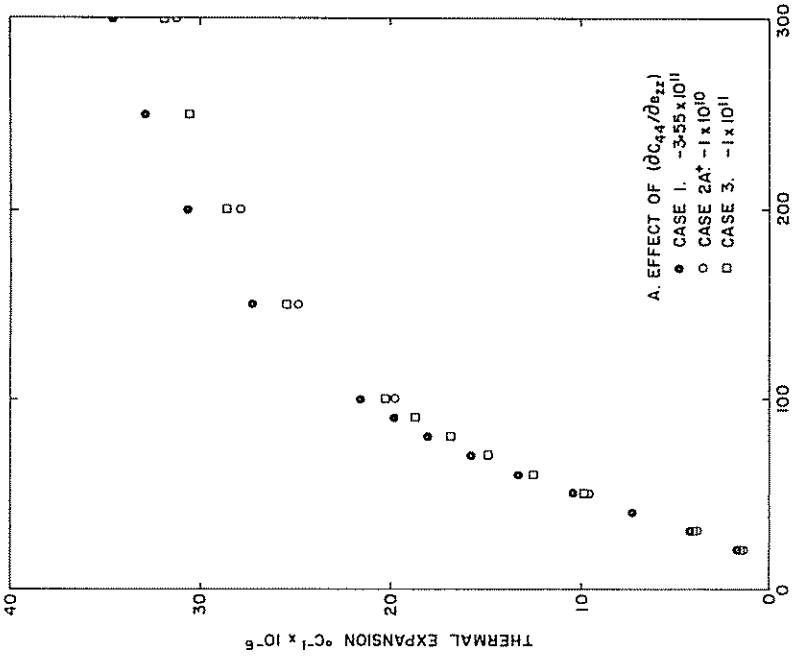


Fig. 3. Comparison of theoretical values of $\alpha_c$. Low temperature. Parametric variation.

to vibration amplitudes is small[14]. This is examined below.

3. The difference is due to deviations of the real vibration spectrum[25] from the continuum model[12]. The true spectrum [16] has additional peaks in the density of states curve which would increase the expansion coefficient at high temperature, and there is a change in elastic constants with temperature.

Clearly items two and three do have some effect, but it is probable that item one is important and on the assumption that it dominates Table 5 can be constructed and compared with the simple estimates of $[\gamma_p]_{zz}$

3.1.2 *In-plane transverse*

The same expression holds with $V_L$ replaced by $V_T$ and $C_{11}$ by $\frac{1}{2}(C_{11}-C_{12})$.

The correction to the out-of-plane contribution is only significant at high temperatures, where much previous experience[13] of calculation in the Komatsu model has shown that a two dimensional approximation is valid. Setting $\tau = 0$, $(\partial C_{44}/\partial e_{zz}) = 0$ in (15) leads to

$$\Delta\alpha_C{}^L = -\frac{\pi S_{33} k \sigma_m{}^2}{\rho d V_L{}^2}\left(\frac{T}{\theta_L}\right)^2 . J_3(\theta_L/T)\left[\frac{\partial C_{11}}{\partial e_{zz}}\right]$$

$$= 3{\cdot}8\times 10^{-6}\left(\frac{T}{\theta_L}\right)^2 J_3(\theta_L/T) \qquad (16)$$

Table 5. Approximate estimate of $[\gamma_p]_{zz}$ from Fig. 6

| Temp. (°K) | $\alpha_c$ (°C$^{-1}$) | Difference ($\alpha_c$ − out-of-plane contribution) $\Delta$ °C$^{-1}$ | $[\gamma_{1\text{ or }2}]_{zz} = \dfrac{\Delta}{\rho S_{33}[C_1(T)+C_2(T)]}$ |
|---|---|---|---|
| 523 | $29{\cdot}0\times 10^{-6}$ | | |
| 1023 | 31·3 | $1\times 10^{-6}$ | −0·015 |
| 1773 | 35 | 4 | 0·045 |
| 2773 | 39 | 8 | 0·09 |

already made. The values in the last column are slightly smaller than the −0·16 obtained from the fit of the out-of-plane mode at low temperatures to yield $\delta^{-1}$ $(\partial\delta/\partial e_{zz})$, but they do suggest 1) to be significant as already surmised. More exact expressions for the in-plane modes contribution to $\alpha_c$ are given below.

3.1.1 *In-plane longitudinal*

$$\Delta\alpha_c{}^L = -S_{33} k\left[\frac{h}{kT}\right]^2 \pi \int_0^{\sigma_m}\int_{-(1/2d)}^{+(1/2d)}$$

$$\frac{\sigma_a\left[\dfrac{\sigma_a{}^2}{\rho}(\partial C_{11}/\partial e_{zz}) + \dfrac{\sin^2\pi d\sigma_z}{\rho\pi^2 d^2}(\partial C_{44}/\partial e_{zz})\right]\exp\left[h/kT\,.\left\{V_L{}^2\sigma_a{}^2 + \dfrac{\tau}{\pi^2 d^2}\sin^2\pi d\sigma_z\right\}^{1/2}\right]}{\left\{\exp\left[h/kT\left(V_L{}^2\sigma_a{}^2 + \dfrac{\tau}{\pi^2 d^2}\sin^2\pi d\sigma_z\right)^{1/2}\right]-1\right\}^2}$$

$$d\sigma_a\,.\,d\sigma_z \qquad (15)$$

where $\theta_L = (hV_L\sigma_m/k)$ and $J_n(\theta_L/T)$ is the Debye integral of order $n$. Similarly the transverse modes contribute

$$\Delta\alpha_C{}^T = -\frac{\pi S_{33} k \sigma_m{}^2}{\rho d V_T{}^2}\left(\frac{T}{\theta_T}\right)^2 J_3(\theta_T/T)\left[\frac{\partial}{\partial e_{zz}}\frac{1}{2}\right.$$

$$\left.(C_{11}-C_{12})\right] = 3{\cdot}0\times 10^{-6}\left(\frac{T}{\theta_T}\right)^2 J_3(\theta_T/T). \qquad (17)$$

Numerical values from these formulae are

shown in Table 6 below, using,

$\theta_L = 2350°K$, $(\partial C_{11}/\partial e_{zz}) = -0{\cdot}16 \times 10^{13}$ dynes/cm$^2$

$\theta_T = 1500°K$, $\partial\frac{1}{2}(C_{11} - C_{12})/\partial e_{zz} = -0{\cdot}05 \times 10^{13}$ dynes/cm$^2$.

The latter values being rough estimates as derived from

$$\left(\frac{1}{\delta} \cdot \frac{\partial \delta}{\partial e_{zz}}\right).$$

It is clear that as required the correction is

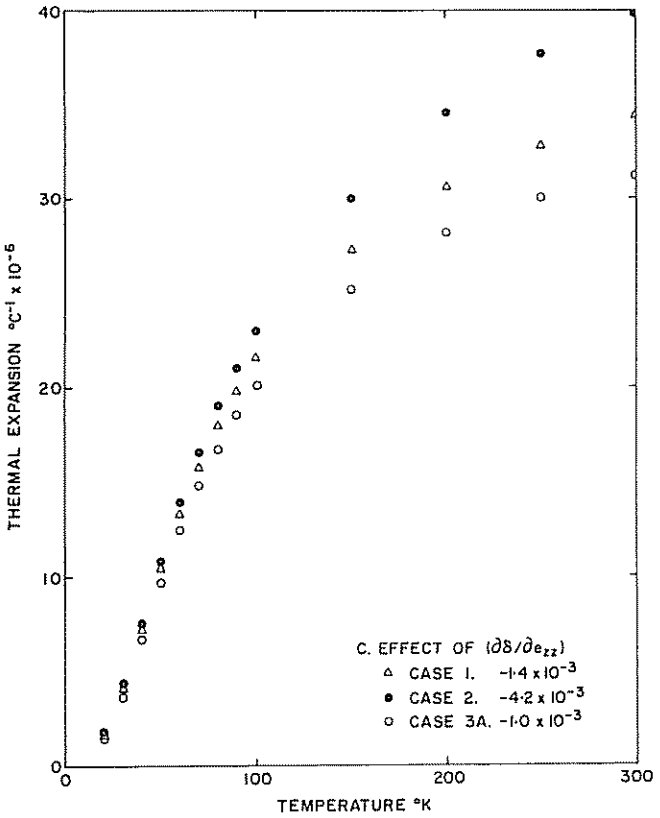


Fig. 5. Comparison of theoretical values of $\alpha_c$. Low temperature. Parametric variation.

Table 6. Estimated contributions to $\alpha_C$ from in-plane vibrations

| Temp. ($T$°K) | $\Delta\alpha_C^T$ °C$^{-1}$ | $\Delta\alpha_C^L$ °C$^{-1}$ | Total correction to $\alpha_C$ (°C$^{-1}$) |
|---|---|---|---|
| 0 | 0 | 0 | 0 |
| 300 | $0{\cdot}64 \times 10^{-6}$ | $0{\cdot}42 \times 10^{-6}$ | $1{\cdot}09 \times 10^{-6}$ |
| 1000 | 1·36 | 1·52 | 2·88 |
| 1500 | 1·44 | 1·42 | 3·16 |
| 2000 | 1·47 | 1·80 | 3·27 |
| 2500 | 1·48 | 1·83 | 3·31 |
| 3000 | 1·50 | 1·85 | 3·35 |

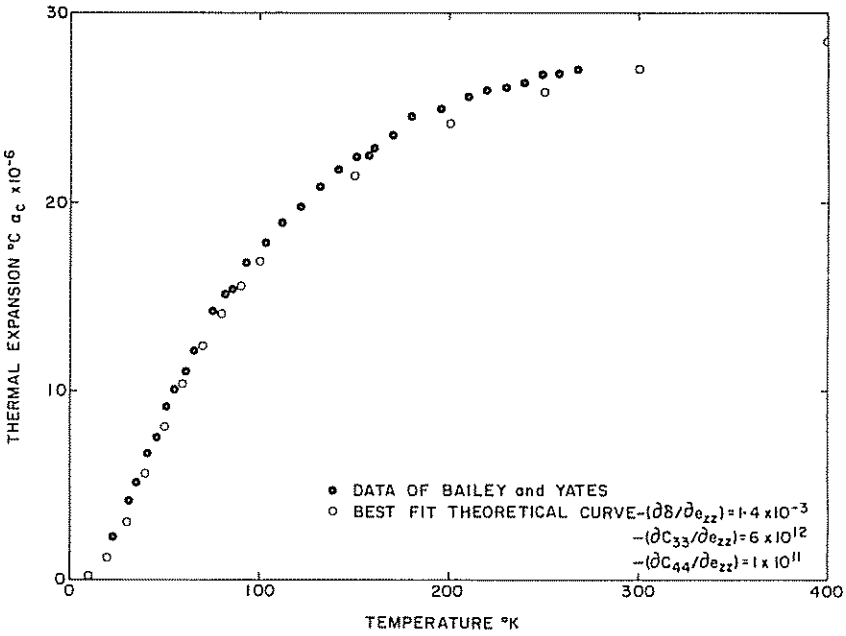


Fig. 6. Fit of theory and experiment for $\alpha_c$ at low temperature.

small at 300°K, and about half the total at say 2500°K.

The out-of-plane optical mode is likely to be much the most important of the optical modes, by analogy with the acoustic modes, in evaluation of $\alpha_c$. Yoshimori and Kitano[16] have shown that this optical mode is essentially two dimensional in character, with a constant density of states between frequencies $5{\cdot}1\,\nu_0$ and $10{\cdot}2\,\nu_0$ (where $\nu_0 = 3{\cdot}46 \times 10^{12}$/sec). The magnitude of the contribution to $\alpha_c$ may be evaluated from equation (14), integrating now from $\sigma_a$ values appropriate to these frequency limits. Since the mode is near two dimensional we can also set $\mu^2 = \tau = 0$. The existing calculations have also shown that $(\partial C_{33}/\partial e_{zz})$ is the dominant anharmonic coefficient in the out-of-plane mode, so we neglect $(\partial\delta/\partial e_{zz})$ and $(\partial C_{44}/\partial e_{zz})$ by comparison. On performing the integrations, we find.

$$\alpha_c^{\text{opt}}(T) = -\frac{S_{33}(\partial C_{33}/\partial e_{zz})h}{4\pi^2\rho d^3\delta T} \left\{\frac{\exp(\theta_1/T) - \exp(\theta_2/T)}{(1-\exp(\theta_1/T))(1-\exp(\theta_2/T))}\right\} \quad (18)$$

where

$$\theta_1 = \left[\frac{2\pi h\delta\sigma_1^2}{k}\right] \text{ and } \theta_2 = \left[\frac{2\pi h\delta\sigma_2^2}{k}\right]$$

$\sigma_1$ and $\sigma_2$ are the values of $\sigma_a$ corresponding to $5{\cdot}1\,\nu_0$ and $10{\cdot}2\,\nu_0$ for the out-of-plane mode estimated from the two-dimensional wave number-frequency relation.

$$\nu^2 = 4\pi^2\delta^2\sigma_a^4.$$

This leads to $\theta_1 = 1860$°K, $\theta_2 = 930$°K. Using $S_{33} = 27{\cdot}5 \times 10^{13}$ cm$^2$/dyne and $[\partial C_{33}/\partial e_{zz}] = -6 \times 10^{12}$ dynes/cm$^2$ results in the values tabulated below.

Table 7. Out-of-plane optical mode contributions to $\alpha_c$

| Temp. (°K) | $\alpha_c^{\text{opt}}(T)$°C$^{-1}$ |
|---|---|
| 300 | $0{\cdot}8 \times 10^{-6}$ |
| 1000 | 2·4 |
| 2000 | 2·9 |
| 3000 | 2·9 |

Again, these are of approximately the correct magnitude to account for the difference between theory and experiment at high temperatures.

3.2 *Basal plane thermal expansion coefficient* $\alpha_a$

It is possible to rewrite equation (7) in the form

$$\alpha_a - (S_{13}/S_{33})\alpha_c = (S_{11}+S_{12})k \sum_{r,p} \left(\frac{h\nu_p}{kT}\right)^2 \frac{\exp(h\nu_p/kT)\cdot[\gamma_p]_{xx}}{[\exp(h\nu_p/kT)-1]^2}. \quad (19)$$

The left hand side of equation (19) may be determined from the experimental data, combined with the known elastic constants. Each side of the equation represents the true thermal expansion of a layer, whereas the observed expansion coefficient of course contains a Poissons ratio effect of $c$-axis expansion. The left hand side of equation (19) is tabulated in Table 8. In the same way as before, we can write approximately.

$$\frac{\alpha_a - (S_{13}/S_{33})\alpha_c}{(S_{11}+S_{12})\rho} = C_1(T)[\gamma_1]_{xx} + C_2(T)[\gamma_2]_{xx} + C_3(T)[\gamma_3]_{xx} = C(T)[\gamma]_{xx} \text{ say} \quad (20)$$

where $C(T)$ is the total specific heat and the $[\gamma_p]_{xx}$ are assumed constant and identical for each mode at high temperatures (which should, as before, be approximately true). Table 8 shows $[\gamma_p]_{xx}$ values obtained in this way, denoted by the column $A$:

The results are surprising in two respects:-

(a) The low value of $[\gamma_p]_{xx}$ at high temperature compared to other solids.

(b) The apparent negative values at low temperatures.

The specific heat component associated with $C_3(T)$ is much the largest at low temperatures, and thus the negative values may be associated with the out-of-plane mode. An alternative explanation is that the ratio $(S_{13}/S_{33})$ is larger than the measured constants indicate. Indeed a value of $S_{13}/S_{33} = -0{\cdot}066$ (compared to $-0{\cdot}012$ as measured) would completely remove the anomalous values of $[\gamma_p]_{xx}$ and leave a pure expansion as expected. Column $B$ in Table 8 is computed in this way, giving $[\gamma_p]_{xx}$ values ranging from zero to 0·90 from low to high temperature respectively. At high temperatures the modes make roughly equal contributions, and the model is almost two dimensional once more. The $[\gamma_p]_{xx}$ is then about unity compared to a value of 4·1 computed from a Morse potential for $-(\partial C_{11}/\partial e_{xx})$.

It is difficult to choose between the two possibilities, a negative contribution to the anharmonicities or an incorrect value for $S_{13}$. We return to this point in the discussion. If the second alternative is correct, then the analysis of $\alpha_c$ also requires a correction of up to 15 per cent.

## 4. DISCUSSION

The main objectives of this study, the derivation of a general model of the thermal expansion of a graphite crystal and the application of the semi-continuum model have been achieved. It has been shown that the hexagonal axis expansion coefficient can be fitted in detail using reasonable anharmonic coefficients with the anticipated magnitudes. Corrections for the in-plane contribution and out-of-plane optical mode to $\alpha_c$ are evaluated.

The expansion coefficient parallel to the layers can only be analysed by the theory since no independent estimate of the approximate anharmonicities has been made. The examination suggests either that one of the vibrational modes at least has $[\gamma_p]_{xx}$ values of the opposite sign to usual or that the presently accepted value of $S_{13}$ is seriously in error. The occurrence of unusual $\gamma$-values has been assigned to transverse vibrations in other studies[8], but it is not possible to make a firm decision.

Table 8. True basal plane expansion and anharmonic coefficient $[\gamma_p]_{xx}$

| Temp. (°K) | Basal expansion $[\alpha_a - (S_{13}/S_{33})\alpha_c]$ | Total specific heat $C(T)$ cal/g/°C | $[\gamma_p]_{xx}$ $A$ | $B$ |
|---|---|---|---|---|
| 45 | $-0{\cdot}416 \times 10^{-6}$ | 0·0087 | | 0·00 |
| 100 | −0·93 | 0·033 | | 0·00 |
| 150 | −1·01 | 0·064 | | 0·020 |
| 200 | −1·13 | 0·099 | | 0·039 |
| 250 | −0·95 | 0·137 | | 0·050 |
| 300 | −1·18 | 0·174 | −0·087 | 0·21 |
| 273 | −1·20 | 0·250 | −0·030 | 0·45 |
| 523 | −0·09 | 0·302 | −0·038 | 0·55 |
| 773 | +0·73 | 0·387 | +0·24 | 0·73 |
| 1023 | +1·14 | 0·429 | +0·34 | 0·80 |
| 1273 | +1·36 | 0·460 | +0·38 | 0·83 |
| 1773 | +1·153 | 0·513 | +0·38 | 0·82 |
| 2273 | +1·61 | 0·513 | +0·40 | 0·87 |
| 2773 | +1·63 | 0·513 | +0·41 | 0·90 |

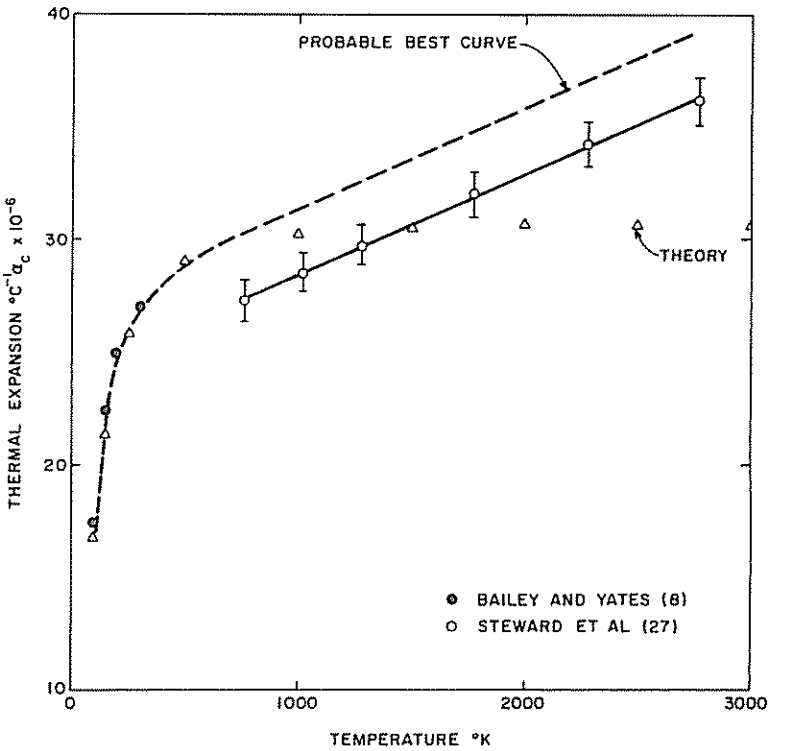


Fig. 7. Fit of theory and experiment—high temperature.

Three recent pieces of work are relevant to these considerations:-

(a) The observations of a marked decrease in $\alpha_c$ following neutron irradiation, accompanied by a change in sign of $\alpha_a$[21].

(b) The observations of changes in $\alpha_c$ with perfection in pyrolytic graphite, recently made by Pellegrini *et al.*[27]. In this case $\alpha_c$ is generally less, the less perfect the graphite, i.e. the larger the *d*-spacing. $\alpha_a$ is not measurably affected.

(c) The observation of wide variations in $\alpha_c$ between different carbonaceous materials reported by Kellet *et al.*[28]. The variations found here are complex for $\alpha_c$, generally showing smaller $\alpha_c$ above 450°C with decreasing perfection. There is evidence in this work that in hemicellulose carbons with $p \approx 1$, either a high $\alpha_c(32 \pm 2{\cdot}5 \times 10^{-6}/°C)$ can be observed at low temperatures or a rather low $\alpha_c(28 \times 10^{-6}/°C)$ independent of temperature. A satisfactory theory would account for all these observations.

In the case of irradiation at temperatures where the *d*-spacing is increased more than about 3 per cent[26] the $S_{33}$ may be markedly increased as may also the $S_{44}$. It is probable that $(\partial C_{33}/\partial e_{zz})$ and $(\partial C_{44}/\partial e_{zz})$ are reduced. $(\partial\delta/\partial e_{zz})$ may be changed in the same direction but it is already rather small. No detailed measurements of $\alpha_c$ as a function of temperature in this condition exist, to which the theory may be fitted, but it is probable that calculations could be made assuming $(\partial\delta/\partial e_{zz})$ to be zero, $S_{33}$ and $S_{44}$ increased by up to about three times and fitting a value of $(\partial C_{33}/\partial e_{zz})$. This is an area for future study. The change in $\alpha_a$ was most simply explained on the theory of Riley[10] as the reduction of the Poisson ratio contraction due to the *c*-axis expansion so that only the positive true thermal expansion of the layer was visible. The present analysis and the latest value of $S_{13}$ does not support this, since they suggest a true negative component of the basal coefficient. Again further studies are necessary.

Pellegrini *et al.* found a decrease in $\alpha_c$ which is presumably explicable, as above, but could not measure a change in $\alpha_a$, so that no conclusions can be drawn. No values of $\alpha_a$ are obtained from the studies of Kellet *et al.* [18].

It is to be hoped that the values of anharmonic coefficients obtained, together with further calculations on interatomic forces, particularly in the layer planes will stimulate studies of problems such as thermal expansion and phonon-phonon interaction.

*Acknowledgments*—I am indebted to Dr. H. P. Rooksby (G.E.C., Wembley) for permission to quote the results of Ref. [28], and also to Dr. B. Yates of Univ. of Salford for his results prior to publication. The Central Technical Services of the U.K.A.E.A. (Mr. M. Toes) programmed calculations. This work is published by permission of the Managing Director of the Reactor Group, U.K.A.E.A., and was supported in part by the U.S.A.E.C. on contract AT(30-1)-1710, during the stay of B.T.K. at Penn. State University in the summer of 1969.

## REFERENCES

1. Nelson J. B. and Riley D. P., *Phys. Soc.* **57**, 477 (1945).
2. Steward E. G. and Cook B. P., *Nature* **185**, 78 (1960).
3. Steward E. G., Cook B. A. and Kellet E. A., *Nature* **187**, 1015 (1960).
4. Kellet E. A. and Richards B. P., *J. Nucl. Mater.* **12**, 184 (1964).
5. Mason I. B. and Knibbs R. H., *J. Nucl. Energy* A/B. **18**, 311 (1964).
6. Martin W. H. and Entwistle F., *J. Nucl. Mater.* **10**, 1 (1963).
7. Sutton A. and Howard V. C., *J. Nucl. Mater.* **7**, 58 (1962).
8. Bailey A. and Yates B., *J. Appl. Phys.* To be published.
9. Entwistle F., *Phys. Rev. Letters* **2**, 236 (1962).
10. Riley F. P., *Phys. Soc.* **57**, 486 (1945).
11. Kittel C., *Introduction to Solid State Physics.* Wiley, New York (1956).
12. Komatsu K., *J. Phys. Soc. Japan* **10**, 346 (1964); *Phys. Chem. Solids* **6**, 380 (1958); *Phys. Chem. Solids* **25**, 404 (1963).
13. Kelly B. T., *Carbon* **5**, 247 (1967); *ibid.* **6**, 41 (1968); *Ibid.* **6**, 485 (1968).

14. Kelly B. T., *J. Nucl. Mater.* **24**, 210 (1964).
15. Reynolds W. N., *The Physical Properties of Graphite*. Elsevier, New York (1968).
16. Yoshimori A. and Kitano Y., *J. Phys. Soc. Japan* **2**, 352 (1956).
17. Girifalco L. A. and Lad R. A., *J. Chem. Phys.* **25**, 693 (1956).
18. Agranovich V. and Semenov L. P., *J. Nucl. Energy* A/B **11**, 141 (1964).
19. Crowell D., *J. Chem. Phys.* **16**, 1407 (1957).
20. Drickamer H. G., Lynch R. W., Clendenen R. L. and Perez-Albuerne E. A., *Solid State Phys.* **19**, 135 (1966).
21. Kelly B. T. and Duff M. J., *Carbon*. **1**, 77 (1970).
22. Thrower P. A., *Chemistry and Physics of Carbon* (Edited by P. L. Walker, Jr.), Vol. 5. Marcel Dekker, New York (1969).
23. Dolling G. and Brockhouse B. N., *Physica* **128**, 1120 (1962).
24. Komatsu K., and Nagamiya T., *J. Phys. Soc. Japan* **6**, 438 (1951).
25. Kelly B. T., *Chemistry and Physics of Carbon* (Edited by P. L. Walker, Jr.) Vol. 5. Marcel Dekker, New York (1969).
26. Kelly B. T., Martin W. H. and Nettley P. T., *Proc. Roy. Soc.* A 240, **260**, 37 (1966).
27. Pellegrini G., Moulaert M. and Zubani I., *Presented at the the Ninth Biennial Carbon Conference*, Boston, U.S.A. (1969).
28. Kellet B. P. *et al.* To be published.

*Note added in proof*

The anharmonic coefficient for strains in the basal plane $e_{x,x}$, is here defined as $1/\nu \cdot (\delta\nu/\delta e_{x,x})$, the strain $e_{x,x}$ being measured along any straight line in the basal plane. It is possible to use the areal strain $\epsilon^1 = 2e_{x,x}$, (since $e_{x,x} = e_{yy}$) as is done by Ramji Rao and Srinivasan. (*Phys. Stat. Solidi* **29**, 865 (1968)), in place of $e_{x,x}$ since the layer planes are isotropic. In isotropic crystals $\gamma = 1/\nu \cdot \delta\nu/\delta(\Delta V/V_0)$, where $\Delta V/V_0 = 3e_{x,x}$, and care must be taken in comparing $\gamma$-values from different sources if these are used to discuss the nature of the bonding. The change of properties of the layer is equally well defined by $e_{x,x}$ or $\epsilon^1$, so that no problem of analysis arises.